

# Spin Hall magnetoresistance and spin orbit torque efficiency in Pt/FeCoB bilayers

Alessandro Magni<sup>1</sup>, Vittorio Basso<sup>1</sup>, Alessandro Sola<sup>1</sup>, Gabriel Soares<sup>1</sup>, Nicola Meggiato<sup>1,2</sup>, Michaela Kuepferling<sup>1</sup>, Witold Skowroński<sup>3</sup>, Stanisław Łazarski<sup>3</sup>, Krzysztof Grochot<sup>3</sup>, Mehran Vafaei Khanjani<sup>4</sup>, Juergen Langer<sup>4</sup>, Berthold Ocker<sup>4</sup>

<sup>1</sup> Istituto Nazionale di Ricerca Metrologica, Torino, Italy

<sup>2</sup> Politecnico di Torino, Torino, Italy

<sup>3</sup> AGH University of Science and Technology, Institute of Electronics, Kraków, Poland

<sup>4</sup> Singulus Technologies AG, Kahl am Main, Germany

**The spin Hall magnetoresistance (SMR) of Pt/FeCoB bilayers with in-plane magnetocrystalline anisotropy was analysed with respect to a second order effect in the sensing current which acts, through the spin Hall effect in Pt, as a torque on the magnetization of the ferromagnetic layer and changes slightly its configuration. This leads to a small current dependent shift of the SMR curves in field that allows, in structures with a multidomain state (e.g. Hall bars), the determination of the sign of the magnetic remanence. The SMR measurements were performed as a function of the Pt thickness and the spin Hall angle, the diffusion length and the field-like and damping like SOT efficiency were determined. The results were compared with the values obtained from harmonic Hall voltage and SOT-ferromagnetic resonance (FMR) measurements and show a good agreement.**

*Index Terms*—spin Hall magnetoresistance, spin Hall effect, spin orbit torque, FeCoB, Pt

## I. INTRODUCTION

The current induced spin-orbit-torque (SOT) [1]–[4] is the physical phenomenon by which a magnetic moment current (or spin current), generated by a heavy metal (HM) layer, induces a magnetic torque on a side ferromagnetic (FM) layer. The magnetic torque is able to induce dynamical phenomena in the ferromagnet including magnetization oscillations [5] and switching [6]. Such bilayers are therefore considered as promising elements to be applied as microwave generators and as magnetic bits of classical non-volatile memories as well as of modern artificial neural networks [1].

One of the key features of the HM/FM bilayers to be used as magnetic bits in magnetic memories or sensors is the possibility to either write or read the magnetic state by electric means. Here the possibilities depend much upon the anisotropy type realized in the FM layer. With perpendicular-to-plane magnetic anisotropy (PMA) the writing is performed by the precessional toggle switching between positive and negative saturation magnetization [7]. The reading of the magnetization state is possible by a voltage measurement through the anomalous Hall effect of the FM. While the development of magnetic memories is nowadays oriented towards the PMA [8]–[10], in-plane anisotropy is still of interest, also for applications such as sensors, since they do not require ultrathin magnetic films and are characterized by more stable and lower noise signals [11]–[13]. With in-plane anisotropy the writing is performed either by the precessional or the damped switching, but the reading is more difficult. One possibility is to introduce a second interface made of a tunnel junction between the FM layer and another ferromagnetic layer with fixed magnetization direction [14]. In this way the reading is performed by means

of the tunnel magnetoresistance (TMR) between the two ferromagnets. Such a device not only becomes rather complex from the point of view of the preparation, but it also requires to optimize SOT together with the TMR. Alternatives for reading the magnetization state and evaluating the SOT efficiency would be welcome.

Recently Liu et al. [15] have suggested that the magnetization state, which is written by a current pulse, could be read by an alternating sense current pulse of lower amplitude. By the comparison of the magnetoresistance signal obtained by the two current pulses of opposite sign the spin orbit field and the SOT efficiency can be evaluated. In their work, the latter is obtained from magnetization switching experiments (i.e. magnetization reversal by the current in the HM) in Hall bars, an experiment which depends on the magnetization or domain configuration and dynamics in the Hall bar and on the strength of the SOT. However, a detailed analysis of the relation between magnetization state and SOT is missing.

We point out that: 1) The magnetoresistance measurements are performed in a structure (Hall bar) which is not a bistable unit but the magnetization  $M$  is a hysteretic function of the applied field, i.e. the magnetization reversal occurs by nucleation and propagation of domain walls. 2) The mechanism proposed in Ref. [15] is a second order effect in the current. The spin current generated by the spin Hall effect and injected in the ferromagnetic layer induces a change of the magnetization configuration by SOT, which causes a shift of the SMR curve as a function of magnetic field. We show here that a detailed analysis of the spin Hall magnetoresistance (SMR) curves as a function of field and electric current shows the influence of SOT on the magnetization state. This analysis may help to read the remanence state and to investigate the performance of SOT even if the spin current generated by the spin Hall effect

Corresponding author: M. Kuepferling (email:m.kuepferling@inrim.it).

is not large enough to reverse the magnetization direction in an extended structure, such as a Hall bar.

## II. EXPERIMENTAL

In this paper we performed an experimental investigation of the SMR [16] in Pt/FeCoB bilayers, in order to shed a clearer light upon the mechanism envisaged by Liu et al. [15]. We compared the results with the harmonic Hall voltage analysis and SOT-induced ferromagnetic resonance (FMR) performed in the same heterostructures in order to validate the approach.

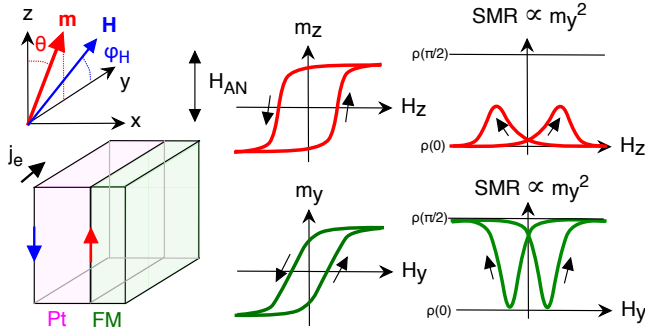


Fig. 1. Left. Scheme of the heterostructure composed by a spin Hall metal (usually a heavy metal; here Pt) and a ferromagnetic metal (here Fe<sub>60</sub>Co<sub>20</sub>B<sub>20</sub>). The electric current, along  $y$ , generates in the metal a current of magnetic moments along  $z$  flowing along  $x$ :  $j_{x,M_z} = \theta_{SH}(\mu_B/e)j_{e,y}$  where  $\theta_{SH}$  is the spin Hall angle (positive for Pt and negative for W and Ta). The FM has a magnetic anisotropy along  $z$ . Right: illustration of the relation between the magnetization curves and the SMR signal for both a magnetic field applied along  $z$  (red curves) and  $y$  (green curves).

The samples are HM/FM heterostructures with HM=Pt (wedge 4-19nm) and FM=Fe<sub>60</sub>Co<sub>20</sub>B<sub>20</sub> (2nm) deposited by Singulus Technologies AG using magnetron sputtering. All samples were annealed for 2h at 310°C in a magnetic field of 1 T in order to develop an in-plane magnetic anisotropy along the  $z$ -axis (see Fig. 1). For all measurements the films were patterned into  $\mu\text{m}$ -size Hall bars/crosses (SMR-bar: length 70  $\mu\text{m}$  along  $y$  and width 6  $\mu\text{m}$  along  $z$ ; SOT-FMR-cross: length 20  $\mu\text{m}$  along  $z$  and width 30  $\mu\text{m}$  along  $y$ ; harmonic Hall-cross: length 30  $\mu\text{m}$  along  $z$  and width 10  $\mu\text{m}$  along  $y$ ) using optical lithography and ion-beam etching with Ti/Au contact pads.

Magneto-optic Kerr effect measurements (MOKE) were performed by recording the magnetic contrast of the Hall bar as a function of the applied magnetic field. This contrast is related to the normalized component of the magnetization in the plane of incidence [17], and we defined the technical value of  $M_S$  as the recorded light intensity value at the maximum applied field  $\mu_0 H = 10$  mT. The setup includes a Hamamatsu C9100 camera equipped with a 50X objective (N.A.=0.55). For the application of the magnetic field along the  $y$  and  $z$  directions we employed a calibrated four-pole electromagnet.

SMR measurements were performed following the protocol of Ref. [15]. For the four-point resistance measurement a Keithley 6221 source was used that provides 60 ms current pulses triggered together with a Keithley 2182A nanovoltmeter for the voltage acquisition. The magnetic field was calibrated by means of a Hall probe in a four-pole electromagnet, both in the  $y$  and  $z$  directions.

SOT-FMR measurements were performed by injecting an amplitude-modulated radio frequency (RF) current of a power of 16 dBm with frequencies between 4-12 GHz to the Hall-cross structure. The mixing voltage was measured by a lock-in amplifier synchronized to the RF signal.

The harmonic Hall measurement was performed at a low frequency signal of 284 Hz and 1 V. The first and second harmonic signal was detected via a lock-in amplifier, dependent on the in-plane angle  $\varphi_H$  between the current and the magnetic field.

## III. RESULTS AND DISCUSSION

The SMR signal is the change of the electric resistivity of the HM with the angle of the magnetization of the FM layer with respect to a fixed electric current direction, induced by the spin Hall effect. The SMR theory [4], [18], [19] provides the equation

$$\frac{\varrho(\theta) - \varrho(0)}{\varrho(0)} = \Delta \hat{\varrho}_{\text{SMR}} \sin^2 \theta \quad (1)$$

where  $\Delta \hat{\varrho}_{\text{SMR}}$  is a coefficient to be determined. When this equation is applied to a multi domain magnetic state one can write

$$\frac{\varrho(\theta) - \varrho(0)}{\varrho(0)} = \Delta \hat{\varrho}_{\text{SMR}} m_y^2 \quad (2)$$

Therefore, the SMR provides a method to evaluate the component of the magnetization along  $y$ ,  $m_y^2$ . The sketch in Fig.1 shows the hysteresis loops with magnetic field along  $z$  and  $y$  and the corresponding components of  $m_y^2$  for the two processes. The inversion of the magnetization along  $z$  corresponds to the acquisition of a small component along  $y$  at the coercive field. This is due to the fact that the magnetization process involves the rotation of magnetic domains and the motion of domain walls that give an overall contribution to the magnetization along  $y$  even if the driving field is along  $z$ . Fig.2 shows the comparison between MOKE loops with magnetic field along  $z$  and along  $y$ . The loop shape along the  $z$ -axis is more rectangular and indicates the magnetic easy anisotropy axis. With the field along  $y$  the hysteresis loop is still present but it has lower coercivity and it indicates that the magnetization process is perpendicular to the anisotropy direction. If the SMR is measured along the two magnetization processes one obtains the plots of Fig.2 bottom panel. It is clearly visible that, while the process along  $y$  is able to span the full range of the SMR, the resistivity for the process along  $z$  increases only in correspondence of the coercive fields.

The SMR is a straightforward method when the FM layer is an insulator [20], while with a metallic FM, in which the testing electric current is not confined in the HM layer only, it is accompanied by additional effects, such as the anisotropic magnetoresistance (AMR) of the FM. However in our case the ratio of the FM/HM resistivities is a factor 10. The contribution to the FM layer to the total resistance is around 3% and the AMR of FeCoB is around 0.1%, while the SMR of Pt is around 1%. Therefore the contribution of AMR is safely negligible.

The presence of a non perfectly squared loop along  $z$  can be an advantage because it offers the possibility to detect

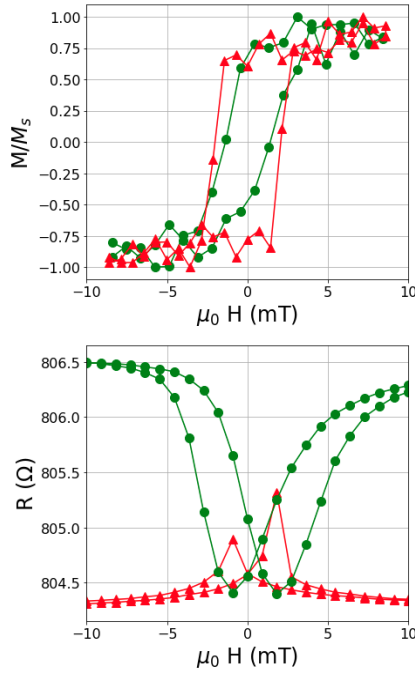


Fig. 2. Comparison between MOKE loop (top panel) and the SMR signal (bottom panel). The MOKE loop along the  $z$  axis (red triangles) is more rectangular and indicates the magnetic easy anisotropy axis with respect to the loop along the  $y$  hard axis (green circles). The SMR signal generated by an electrical current  $I = 1\text{mA}$  is much more pronounced with the field along the  $y$  axis (green circles) where the current is parallel to the field, while it shows a small peak close to the coercivity when the field is along the  $z$  axis (red). Sample Pt thickness  $d_{Pt}=6.1\text{ nm}$ , current density  $j_e = 2.5 \cdot 10^{10}\text{ Am}^{-2}$ .

the magnetization state by means of the SMR even in a configuration in which it would be precluded for a perfect bistable switching. The idea is that the electric current used to sense the SMR necessarily acts as a small torque on the FM magnetization and therefore it slightly alters the original magnetic state, causing a shift of the SMR curves (see Fig.3). However, the effect of the torque depends on both the sign of the current and the sign of the remanence. Considering the torque introduced by the spin Hall effect of Pt (which has a positive spin Hall angle  $\theta_{SH}$  [20]), its effect is explained in the scheme of Fig.4. On the left side of the figure it is shown that positive and negative SOT change the remanent magnetization  $m_r$  in opposite directions. Because of the induced torque the SMR (voltage over current) will have a slight dependence upon the current. On the right side we see the effect of the changed remanence on the SMR curve as a function of the effective field (upper panel) and the current density (lower panel). We find a lower SMR value for negative  $m_r$  and negative SOT, while SMR is increased for positive  $m_r$ , and vice versa. This non linear second order effect can be used to detect the positive or negative magnetic state at remanence.

We now evaluate the torque exerted by the spin Hall effect in the Pt/FM bilayers. The coefficient  $\Delta\hat{Q}_{SMR}$  as a function of the Pt thickness follows the equation [21]

$$\Delta\hat{Q}_{SMR} = \theta_{SH}^2 \frac{1}{x} \frac{\tanh(x) \tanh(x/2)^2}{1 + (G_{Pt}/G_c) \tanh(x)} \quad (3)$$

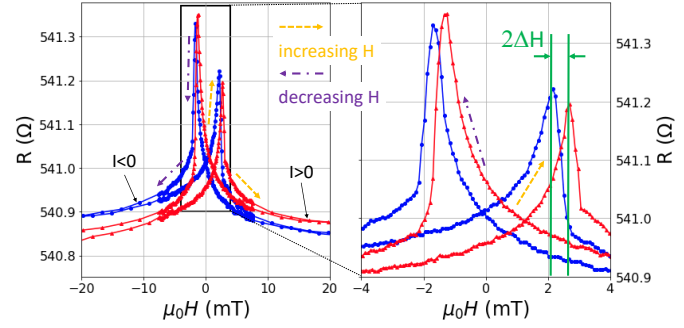


Fig. 3. SMR loops with ( $I = \pm 10\text{mA}$ , Pt thickness  $7.6\text{ nm}$ ) and zoom (right panel) showing the horizontal displacement  $\Delta H$  with respect to positive (red curve) and negative (blue curve) current. The resistance reading discriminates the magnetic states at remanence.

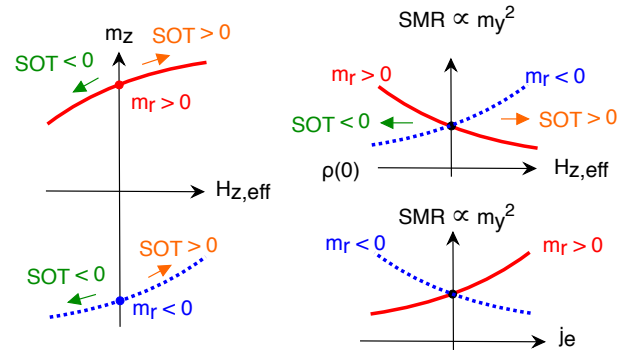


Fig. 4. The scheme illustrates the relation between remanence state and SMR signal. The electric current density  $j_e$  acts through the spin Hall effect as a torque on the magnetization and shifts the magnetization curves.

where  $x = d_{Pt}/l_{Pt}$  is the ratio between the thickness and the diffusion length of Pt,  $\theta_{SH}$  is the spin Hall angle of Pt,  $G_{Pt} = \sigma_{e,Pt}/l_{Pt}$  is the effective conductance of Pt and  $G_c$  is the finite conductance at the interface [21]. The fit of the measured data (see Fig.5) provides  $G_c = 1 \cdot 10^{16}\text{ }\Omega^{-1}\text{m}^{-2}$ ,  $\theta_{SH} = 0.14$ ,  $l_{Pt} = 1.1 \cdot 10^{-9}\text{ m}$ . It is therefore possible to compute the damping like SOT efficiency [4] as

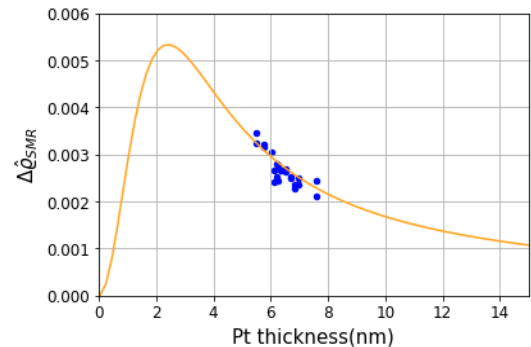


Fig. 5.  $\Delta\hat{Q}_{SMR}$  as a function of Pt thickness. Blue points: measured data. Yellow curve: fit following Eq.3 using  $G_c = 1 \cdot 10^{16}\text{ }\Omega^{-1}\text{m}^{-2}$ ,  $\theta_{SH} = 0.14$ ,  $l_{Pt} = 1.1\text{ nm}$ .

$$\xi_{DL} = \theta_{SH} \frac{\tanh(x) \tanh(x/2)}{1 + (G_{Pt}/G_c) \tanh(x)} \quad (4)$$

which in the range  $d_{Pt} = 5 - 7$  nm turns out to be  $\xi_{DL} = 0.117$ .

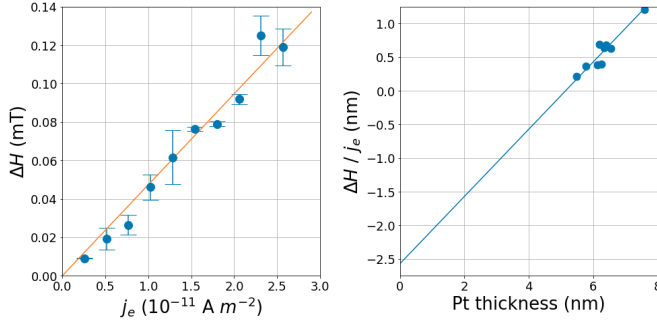


Fig. 6. SMR peaks displacements as a function of the current (left: sample Pt thickness 5.8 nm) and as a function of Pt thickness (right:  $I = 10$  mA). Left: a linear increase of the SMR peaks shift with the current density is observed. Right: The  $y$ -axis intercept of the line fit with slope 1/2 delivers, according to Eq.7, the SOT efficiency.

However, the SOT effective field  $\mathbf{H}_{SOT}$  is subdivided into a field-like and a damping-like part as

$$\mathbf{H}_{SOT} = H_{DL} \mathbf{m} \times \hat{\mathbf{z}} + H_{FL} \hat{\mathbf{z}} \quad (5)$$

where  $\mathbf{m}$  is the reduced magnetization of the FM and  $\hat{\mathbf{z}}$  is the direction of the moment injected by the spin Hall layer. The two components are given by

$$H_{FL/DL} = \frac{[(\hbar/2)/e]j_e}{\mu_0 M_s d_{FM}} \xi_{FL/DL} \quad (6)$$

where  $M_s$  is the saturation magnetization and  $\xi_{FL}$  and  $\xi_{DL}$  are the field-like and damping-like efficiencies, respectively. The effective field  $H_{eff}$  acting on the magnetization becomes the sum of the applied field, the spin orbit field and the magnetic field generated by the current  $j_e$ ,  $H_{Oe,z}$  (the Oersted field). As shown in Fig.6, the displacement of the SMR curves, applying the field along  $z$ , is a function of  $j_e$ . The observed field displacement  $\Delta H$  can be attributed to the effective field and, estimating the spin orbit field along  $z$  by the field-like component only, we obtain  $H_{eff,z} = H_z + H_{FL} + H_{Oe,z}$ . Therefore we get the displacement

$$\frac{\Delta H}{j_e} = -\frac{(\hbar/2)/e}{\mu_0 M_s d_{FM}} \xi_{FL} + \frac{d_{Pt}}{2} \quad (7)$$

From Fig.6 we can derive  $\xi_{FL} = 0.019$  with the saturation magnetization chosen equal to the effective magnetization obtained from the FMR measurements (see below)  $\mu_0 M_s = \mu_0 M_{eff} = 1.2$  T.

To validate the SOT parameters obtained, we performed independent SOT-FMR measurements followed by an angular dependent harmonic Hall voltage analysis of the Pt/FeCoB bilayers. First, SOT-FMR were determined for different Pt thickness, resulting in the frequency vs. in-plane magnetic field relation, modelled using the Kittel formula [22], and the FMR linewidth as a function of frequency - Fig. 7(a-b). Thus, the

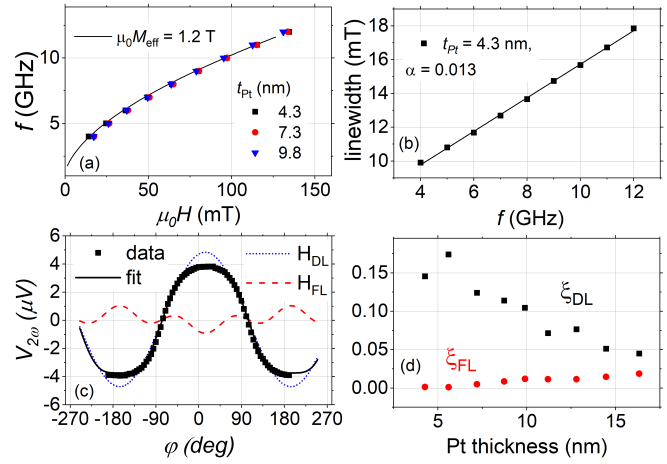


Fig. 7. Spin-orbit torque induced ferromagnetic resonance and harmonic Hall voltage measurements of Pt/FeCoB bilayers. Frequency vs. magnetic field dependence modelled using the Kittel formula (a), linewidth vs. frequency dependence resulting in a magnetization damping coefficient calculation (b). Example of the angular dependence of the second harmonic Hall voltage ( $V_{2\omega}$ ) modelled using Eq. 8 (c) and the damping-like and field-like SOT efficiencies vs. Pt thickness.

values of the effective magnetization  $\mu_0 M_{eff} = 1.2$  T was obtained and magnetization damping between  $\alpha = 0.013 - 0.015$  depending on the Pt thickness.

Afterwards, we determined the SOT components using the analysis of the harmonic Hall signals, based on the approach proposed by Avci et al. [23]. To do so, we first measured the resistivity dependence on Pt thickness using the four-point method [3], which decreases from  $\rho_{Pt} = 52 \cdot 10^{-8} \Omega \text{ m}$  for  $d_{Pt} = 4.5$  nm down to  $24 \cdot 10^{-8} \Omega$  for 14 nm. Then, the first and second harmonic Hall signals were determined as a function of the in-plane magnetic field angle ( $\varphi_H$ ) for different field magnitudes ( $H$ ) - Fig. 7(c) - which was then modelled using the formula:

$$V_{2\omega} = -A \cos \varphi_H \cos 2\varphi_H - B \cos \varphi_H \quad (8)$$

where  $A = \frac{V_P H_{FL}}{H}$ , is proportional to the planar Hall voltage  $V_P$  and the field-like effective field  $H_{FL}$  and  $B = \left( \frac{V_A H_{DL}}{2H_{eff}} - V_{ANE} \right)$  is proportional to the anomalous Hall voltage  $V_A$  and the damping-like effective field  $H_{DL}$ . The anomalous Nernst contribution  $V_{ANE}$  was found negligible. Modelling the  $A$  vs.  $1/H$  and  $B$  vs.  $1/H_{eff}$  dependencies with linear functions results in  $H_{FL}$  and  $H_{DL}$ , which was then converted into the spin orbit torque efficiency using Eq.6. The dependencies of  $\xi_{DL}$  and  $\xi_{FL}$  on  $d_{Pt}$  are presented in Fig. 7(d). Both SOT efficiencies calculated this way agree well with the values obtained from the SMR measurements in the range  $d_{Pt} = 5-7$  nm.

#### IV. CONCLUSIONS

We performed measurements of SMR in metallic heterostructures consisting of Pt/FeCoB with various Pt thicknesses and magnetocrystalline anisotropy in the film plane. Although the sensing current is not limited to the Pt layer

due to the finite resistivity of the FM layer, the resistivity measurement can be almost exclusively ascribed to the SMR effect due to the large difference of the resistances and the AMR and SMR effects. The analysis of the SMR curves shows a second order dependence on the sensing current: the spin current generated through the spin Hall effect in the HM causes a torque on the magnetization of the FM layer and changes slightly the magnetization state, which is reflected in the SMR measurement. In the measured Hall bars, the magnetocrystalline anisotropy direction is perpendicular to the current direction, i.e. along the Hall bar. Therefore, the SMR has a low resistance state when the magnetization is aligned with the easy anisotropy axis and a high resistance state when the magnetization is aligned with the hard anisotropy axis. Due to the fact that the SMR is proportional to the square of the component of the magnetization in the hard direction, any slight change in this component is reflected in the SMR signal. In a structure with a multidomain state, where the magnetization curve has a slope at remanence, this opens up the possibility to sense the magnetization state (positive or negative remanence) by changing from positive to negative current and to perform a magnetization reading. On the other hand it allows for the determination of the SOT efficiencies by determining a) the SMR change (damping like torque; vertical shift of the SMR curve) and b) the effective SOT field causing a displacement of the SMR curve (field like torque; horizontal shift).

#### ACKNOWLEDGMENTS

This project 17FUN08 TOPS has received funding from the EMPIR programme co-financed by the Participating States and from the European Union's Horizon 2020 research and innovation programme. WS acknowledges National Science Centre Grant No. UMO-2015/17/D/ST3/00500, Poland. KG and SŁ acknowledge National Science Centre in Poland Grant UMO-2016/23/B/ST3/01430 (SPINORBITRONICS). Microfabrication was performed at the Academic Centre for Materials and Nanotechnology of AGH.

#### REFERENCES

- [1] B. Dieny, I. L. Prejbeanu, K. Garello, P. Gambardella, P. Freitas, R. Lehdorff, W. Raberg, U. Ebels, S. O. Demokritov, J. Akerman *et al.*, "Opportunities and challenges for spintronics in the microelectronics industry," *Nature Electronics*, vol. 3, no. 8, pp. 446–459, 2020.
- [2] A. Manchon, J. Železný, I. M. Miron, T. Jungwirth, J. Sinova, A. Thiaville, K. Garello, and P. Gambardella, "Current-induced spin-orbit torques in ferromagnetic and antiferromagnetic systems," *Reviews of Modern Physics*, vol. 91, no. 3, p. 035004, 2019.
- [3] M.-H. Nguyen, D. Ralph, and R. Buhrman, "Spin torque study of the spin hall conductivity and spin diffusion length in platinum thin films with varying resistivity," *Physical review letters*, vol. 116, no. 12, p. 126601, 2016.
- [4] C.-F. Pai, Y. Ou, L. H. Vilela-Leão, D. Ralph, and R. Buhrman, "Dependence of the efficiency of spin hall torque on the transparency of p/ferromagnetic layer interfaces," *Physical Review B*, vol. 92, no. 6, p. 064426, 2015.
- [5] L. Liu, T. Moriyama, D. Ralph, and R. Buhrman, "Spin-torque ferromagnetic resonance induced by the spin hall effect," *Physical review letters*, vol. 106, no. 3, p. 036601, 2011.
- [6] L. Liu, C.-F. Pai, Y. Li, H. W. Tseng, D. C. Ralph, and R. A. Buhrman, "Spin-torque switching with the giant spin hall effect of tantalum," *Science*, vol. 336, no. 6081, pp. 555–558, 2012. [Online]. Available: <http://science.sciencemag.org/content/336/6081/555>
- [7] I. M. Miron, K. Garello, G. Gaudin, P.-J. Zermatten, M. V. Costache, S. Auffret, S. Bandiera, B. Rodmacq, A. Schuhl, and P. Gambardella, "Perpendicular switching of a single ferromagnetic layer induced by in-plane current injection," *Nature*, vol. 476, no. 7359, pp. 189–193, 2011.
- [8] K. Garello, F. Yasin, S. Couet, L. Souriau, J. Swerts, S. Rao, S. Van Beek, W. Kim, E. Liu, S. Kundu, D. Tsvetanova, K. Croes, N. Jossart, E. Grimaldi, M. Baumgartner, D. Crotti, A. Fumémont, P. Gambardella, and G. S. Kar, "Sot-mram 300nm integration for low power and ultrafast embedded memories," in *2018 IEEE Symposium on VLSI Circuits*, 2018, pp. 81–82.
- [9] V. Krizakova, K. Garello, E. Grimaldi, G. Sankar Kar, and P. Gambardella, "Cite as," *Appl. Phys. Lett.*, vol. 116, p. 232406, 2020. [Online]. Available: <https://doi.org/10.1063/5.0011433>
- [10] D. Zhu and W. Zhao, "Threshold current density for perpendicular magnetization switching through spin-orbit torque," *Phys. Rev. Applied*, vol. 13, p. 044078, Apr 2020. [Online]. Available: <https://link.aps.org/doi/10.1103/PhysRevApplied.13.044078>
- [11] S. Ingarsson, G. Xiao, S. S. P. Parkin, W. J. Gallagher, G. Grinstein, and R. H. Koch, "Low-frequency magnetic noise in micron-scale magnetic tunnel junctions," *Phys. Rev. Lett.*, vol. 85, pp. 3289–3292, Oct 2000. [Online]. Available: <https://link.aps.org/doi/10.1103/PhysRevLett.85.3289>
- [12] A. Hirohata, K. Yamada, Y. Nakatani, L. Prejbeanu, B. Diény, P. Pirro, and B. Hillebrands, "Review on spintronics: Principles and device applications," *Journal of Magnetism and Magnetic Materials*, vol. 509, p. 166711, sep 2020.
- [13] S. Fukami, T. Anekawa, C. Zhang, and H. Ohno, "A spin-orbit torque switching scheme with collinear magnetic easy axis and current configuration," *Nature Nanotechnology*, vol. 11, no. 7, pp. 621–625, Jul 2016. [Online]. Available: <https://doi.org/10.1038/nnano.2016.29>
- [14] L. Liu, C.-F. Pai, D. C. Ralph, and R. A. Buhrman, "Magnetic oscillations driven by the spin hall effect in 3-terminal magnetic tunnel junction devices," *Phys. Rev. Lett.*, vol. 109, p. 186602, Oct 2012. [Online]. Available: <https://link.aps.org/doi/10.1103/PhysRevLett.109.186602>
- [15] Y.-T. Liu, T.-Y. Chen, T.-H. Lo, T.-Y. Tsai, S.-Y. Yang, Y.-J. Chang, J.-H. Wei, and C.-F. Pai, "Determination of spin-orbit-torque efficiencies in heterostructures with in-plane magnetic anisotropy," *Physical Review Applied*, vol. 13, no. 4, p. 044032, 2020.
- [16] J. Kim, P. Sheng, S. Takahashi, S. Mitani, and M. Hayashi, "Spin hall magnetoresistance in metallic bilayers," *Phys. Rev. Lett.*, vol. 116, p. 097201, Feb 2016. [Online]. Available: <https://link.aps.org/doi/10.1103/PhysRevLett.116.097201>
- [17] A. Hubert and R. Schafer, *Magnetic Domains*. Berlin: Springer-Verlag, 1998.
- [18] M. Althammer, S. Meyer, H. Nakayama, M. Schreier, S. Altmannshofer, M. Weiler, H. Huebl, S. Geprägs, M. Opel, R. Gross *et al.*, "Quantitative study of the spin hall magnetoresistance in ferromagnetic insulator/normal metal hybrids," *Physical Review B*, vol. 87, no. 22, p. 224401, 2013.
- [19] Y.-T. Chen, S. Takahashi, H. Nakayama, M. Althammer, S. T. B. Goennenwein, E. Saitoh, and G. E. W. Bauer, "Theory of spin hall magnetoresistance," *Phys. Rev. B*, vol. 87, p. 144411, Apr 2013. [Online]. Available: <https://link.aps.org/doi/10.1103/PhysRevB.87.144411>
- [20] H. L. Wang, C. H. Du, Y. Pu, R. Adur, P. C. Hammel, and F. Y. Yang, "Scaling of spin Hall angle in 3d, 4d, and 5d metals from Y<sub>3</sub>Fe<sub>5</sub>O<sub>12</sub>/metal spin pumping," *Phys. Rev. Lett.*, vol. 112, p. 197201, 2014.
- [21] J.-G. Choi, J. W. Lee, and B.-G. Park, "Spin hall magnetoresistance in heavy-metal/metallic-ferromagnet multilayer structures," *Physical Review B*, vol. 96, no. 17, p. 174412, 2017.
- [22] C. Kittel, "On the theory of ferromagnetic resonance absorption," *Phys. Rev.*, vol. 73, pp. 155–161, Jan 1948. [Online]. Available: <https://link.aps.org/doi/10.1103/PhysRev.73.155>
- [23] C. O. Avci, K. Garello, M. Gabureac, A. Ghosh, A. Fuhrer, S. F. Alvarado, and P. Gambardella, "Interplay of spin-orbit torque and thermoelectric effects in ferromagnet/normal-metal bilayers," *Phys. Rev. B*, vol. 90, p. 224427, Dec 2014. [Online]. Available: <https://link.aps.org/doi/10.1103/PhysRevB.90.224427>